Molecular Imaging and Biological Evaluation of HuMV833 Anti-VEGF Antibody: Implications for Trial Design of Antiangiogenic Antibodies

Gordon C. Jayson, Jamal Zweit, Alan Jackson, Clive Mulatero, Peter Julyan, Malcolm Ranson, Lynn Broughton, John Wagstaff, Leif Hakannson, Gerard Groenewegen, John Bailey, Nigel Smith, David Hastings, Jeremy Lawrance, Hamied Haroon, Tim Ward, Alan T. McGown, Meina Tang, Dan Levitt, Sandrine Marreaud, Frederic F. Lehmann, Manfred Herold, Heinz Zwierzina

For the European Organisation for Research and Treatment of Cancer (EORTC) Biological Therapeutic Development Group

Background: **Vascular endothelial growth factor (VEGF) is a potent angiogenic cytokine, and various inhibitory agents, including specific antibodies, have been developed to block VEGF-stimulated angiogenesis. We developed HuMV833, a humanized version of a mouse monoclonal anti-VEGF antibody (MV833) that has antitumor activity against a number of human tumor xenografts, and investigated the distribution and biologic effects of HuMV833 in patients in a phase I trial.** ***Methods:*** **Twenty patients with progressive solid tumors were treated with various doses of HuMV833 (0.3, 1, 3, or 10 mg/kg). Positron emission tomography with ^{124}I-HuMV833 was used to measure the antibody distribution in and clearance from tissues. Magnetic resonance imaging was used to measure the vascular permeability surface area product with a first-pass pharmacokinetic model (k_{fp}) to determine tumor vascular permeability.** ***Results:*** **The antibody was generally well tolerated, although the incremental dose, phase I study design, and pharmacodynamic endpoints could not identify the optimum biologically active dose. Antibody distribution and clearance were markedly heterogeneous between and within patients and between and within individual tumors. HuMV833 distribution to normal tissues also varied among patients, but the antibody was cleared from these tissues in a homogeneous fashion. Permeability was strongly heterogeneous between and within patients and between and within individual tumors. All tumors showed a reduction in k_{fp} 48 hours after the first treatment (median = 44%; range = 4%–91%).** ***Conclusions:*** **Because of the heterogeneity in tumor biology with respect to antibody uptake and clearance, we suggest that either intrapatient dose escalation approaches or larger, more precisely defined patient cohorts would be preferable to conventional strategies in the design of phase I studies with antiangiogenic compounds like HuMV833. [J Natl Cancer Inst 2002;94: 1484–93]**

The development of antiangiogenic agents has focused largely on the inhibition of vascular endothelial growth factor (VEGF), one of the most potent angiogenic cytokines. The VEGF cytokine family consists of six different analogues (VEGF, VEGF-B, VEGF-C, VEGF-D, VEGF-E, and placental growth factor). The prototypic member, VEGF, is expressed as one of five different splice variants that contain 121, 145, 165, 189, or 202 amino acids. Two tyrosine kinase VEGF signal-transducing receptors (flt and flk) have been identified, and a third nonsignaling receptor, neuropilin, has also been found *(1).*

A number of strategies have been used to inhibit the biologic activity of VEGF, including antibodies to the cytokine or its signaling receptor *(2,3),* receptor tyrosine kinase inhibitors *(4–7),* and gene therapy approaches, in which the vector produces an antisense molecule or a soluble receptor that acts in a dominant negative manner *(8).* To date, the anti-VEGF antibodies and receptor tyrosine kinase inhibitors evaluated in an early clinical trial *(9)* have shown evidence of antitumor activity. The agents appear to be broadly nontoxic in humans, although there have been some reports of thromboembolic or hemorrhagic events *(2,3,10).*

One anti-VEGF antibody with early preclinical promise is HuMV833, a humanized monoclonal $IgG4_{\kappa}$ antibody that binds $VEGF_{121}$ and $VEGF_{165}$ with a dissociation constant of approximately 10^{-10} *M* and has antitumor activity against a broad spectrum of human tumor xenografts *(11).* In a preclinical evalua-

Affiliations of authors: G. C. Jayson, C. Mulatero, M. Ranson, L. Broughton (Cancer Research UK Department of Medical Oncology), J. Lawrance (Department of Radiology), Christie Hospital NHS Trust, Manchester, U.K.; J. Zweit, J. Bailey, N. Smith, Cancer Research UK/University of Manchester Institute of Science and Technology, Radiochemical Targeting and Imaging Group and Manchester Positron Emission Tomography (PET) Centre, Paterson Institute for Cancer Research, and Christie Hospital NHS Trust, Manchester; A. Jackson, H. Haroon, Division of Imaging Science and Biomedical Engineering, Department of Medicine, University of Manchester, Manchester; P. Julyan, D. Hastings, Manchester PET Centre, Paterson Institute for Cancer Research, and Department of North Western Medical Physics, Christie Hospital NHS Trust; J. Wagstaff, Department of Medical Oncology, Academisch Ziekenhuis Maastricht, Maastricht, The Netherlands; L. Hakannson, Department of Medical Oncology, Linkoping University Hospital, Linkoping, Sweden; G. Groenewegen, Department of Medical Oncology, Universitair Medisch Centrum Utrecht, Utrecht, The Netherlands; T. Ward, A. T. McGown, Cancer Research UK Drug Development Group, Paterson Institute for Cancer Research; M. Tang, D. Levitt, Protein Design Labs, Inc., Fremont, CA; S. Marreaud, F. F. Lehmann, EORTC Data Centre, Brussels, Belgium; M. Herold, H. Zwierzina (Chairman), EORTC Biological Therapeutic Development Group, Innsbruck Universitaetsklinik, Department of Medicine, Innsbruck, Austria.

Correspondence to: Gordon Jayson, F.R.C.P., Ph.D., Cancer Research UK Dept. of Medical Oncology, Christie Hospital NHS Trust, Wilmslow Rd., Withington, Manchester M20 4BX, U.K. (e-mail: Gordon.Jayson@christie-tr.nwest.nhs.uk or GordonJayson@aol.com).

See "Notes" following "References."

tion, the antibody lacked any substantial toxicity in animals treated with up to 30 mg/kg twice a week (Protein Design Labs, Inc.: unpublished data).

Many trials have sought pharmacodynamic endpoints for antiangiogenic agents that lack a dose-limiting toxicity *(12).* However, these trials often use *ex vivo* measurements to evaluate the pharmacodynamic response. To date, studies of the intratumoral concentration of and biologic response to antiangiogenic agents have not been reported. To address these issues, we have used positron emission tomography (PET) imaging with ^{124}I-HuMV833 to determine radioligand uptake and clearance by both tumor and normal tissues. We also determined the *in situ* biologic response by measuring the vascular permeability surface area product, k_{fp}, with dynamic magnetic resonance imaging (MRI) by using a first-pass technique.

Patients and Methods

HuMV833 Development and Preclinical Assessment

HuMV833 development and preclinical evaluations (cross-reactivity with human tissues and pharmacokinetic profile in cynomolgus monkeys) were done by Protein Design Labs, Inc. (Fremont, CA). HuMV833 ($IgG_4\kappa$, molecular mass = 145 kd) is the humanized form of a murine monoclonal antibody, MV833 ($IgG_1\kappa$), that binds to and inhibits VEGF. MV833 was created by using recombinant human $VEGF_{121}$ as the immunogen to elicit an immune response in BALB/c mice. Hybridomas were generated from the spleen cells of these mice according to standard methods *(13).* MV833 was humanized *(14)* at Protein Design Labs, Inc. The cDNA sequences for the MV833 heavy-chain and light-chain variable regions were determined, and sequences of human variable domains that were most similar to those of MV833 were selected to serve as frameworks for the humanized antibody. The complementarity determining regions (CDR) of MV833 were cloned into these human antibody frameworks. With the help of a three-dimensional model that used the predicted amino acid sequence and tertiary structure *(15),* additional human framework amino acid residues were identified that could be altered to preserve the conformation of the MV833 CDRs and thus the binding affinity. The mini exons encoding the humanized MV833 (HuMV833) heavy- and light-chain variable regions were synthesized and then cloned into the vectors designed for the expression of a human gamma-4 heavy chain and a human kappa light chain, respectively. The HuMV833 heavy and light chain expression vectors were cotransfected into the mouse myeloma cell line Sp2/0 (American Type Culture Collection, Manassas, VA) to generate a candidate for the production cell line. One stable transfectant capable of expressing high levels of HuMV833 was selected and adapted to grow in serum-free medium *(16).* The purity of HuMV833 was determined by sodium docecyl sulfate–polyacrylamide gel electrophoresis (8%–16% Tris-Glycine Gel [Invitrogen, Carlsbad, CA]), size exclusion chromatography, and analyses of the residual concentrations of various impurities by size exclusion chromatography–high performance liquid chromatography (SEC–HPLC). The final HuMV833 product was more than 95% pure monomeric antibody (data not shown).

The biologic activity (potency) of HuMV833 was measured by an enzyme-linked immunosorbent assay (ELISA) that quantified the capacity of the antibody to bind VEGF. This ELISA was developed in-house at Protein Design Labs, Inc. (www.pdl.com), and it used recombinant human VEGF (catalog No. 293-VE/CF; R&D Systems, Minneapolis, MN) as the target antigen. The reference and test (HuMV833) antibody binding responses in the ELISA were compared by using parallel line methods, and the potency of the test preparation relative to the reference (relative potency) was calculated. Given the observed inherent assay variability, a range of 70%–130% relative potency was designated equivalent to the reference.

The specificity of HuMV833 was evaluated by determining tissue reactivity with immunohistochemical analysis (protocol No. IM466; Pathology Associates, International, Frederick, MD). HuMV833 (1.25 μg/mL) was used to stain normal human tissues that had been obtained previously via autopsy or surgical biopsy. These tissues were embedded in Tissue-Tek OCT medium, frozen on dry ice, and stored in sealed plastic bags below –70 °C. Tissues were sectioned at 5 μm, allowed to air-dry, and then stored at –70 °C until staining. Slides of the sectioned tissues were fixed in 10% neutral buffered formalin just before staining. This study revealed specific binding (data not shown) to the adrenal capsular and cortical endothelium, perivascular adventitia, glia and endothelium of the brain, perivascular adventitia of the retinal blood vessels of the eye, blood smear granulocytes, ovarian and fallopian tube stromal endothelium, gastric mucosal epithelium, stromal cells of the placenta, and glia and endothelium of the spinal cord. HuMV833 did not bind to the negative control tissue, human cerebellum. The distribution of HuMV833 binding in the various tissues was consistent with normal physiologic processes that may involve VEGF expression. Finally, HuMV833 was shown to inhibit the VEGF-dependent growth of human umbilical vein endothelial cells (HUVEC) in a dose-dependent manner (Protein Design Labs, Inc.: unpublished data).

The preclinical pharmacokinetic profile of HuMV833 was evaluated in cynomolgus monkeys (*Macaca fascicularis*). Animals received HuMV833 diluted in sodium citrate buffer containing 0.01% Tween 80 or placebo (sodium citrate buffer containing 0.01% Tween 80) intravenously, twice a week for 4 weeks. HuMV833 plasma concentrations were measured by specific antibody-captured ELISAs (Protein Design Labs, Inc.), and VEGF165 (R&D Systems) was used as the solid-phase capture reagent. Binding of HuMV833 to the coated well was detected by using horseradish peroxide (HRP)-conjugated sheep anti-human IgG1 mAb (The Binding Site, Ltd., Birmingham, U.K.). To generate a calibration curve, normal human plasma was pooled from 90 individuals and spiked with known concentrations of HuMV833. The data were fitted with a four-parameter logistic regression curve. Regression analyses were used to determine the concentrations of the study samples from the mean of duplicate absorbance values and the calibration curve (SOFTmax PRO Microplate Analysis Software; Molecular Devices, Sunnyvale, CA). The quantitative range of the assay was 50–4500 ng/mL. The ELISA accuracy ranged between 81% and 92%. Precision, an estimate of the variation of reproducibility, of the ELISA was estimated to be less than 13% across the quantitative range. Using a nonlinear, mixed-effects modeling program, NONMEM (NONMEM project group; University of California, San Francisco, CA), the antibody's kinetics were well described by a two-compartment model with a saturable clearance (Michaelis–Menten kinetics).

Overall, within the monkey population, the elimination half-life of HuMV833 was 8–9 days. The clearance of the antibody

showed a nonlinear kinetic, i.e., the clearance decreases as the antibody plasma concentration increases, and this kinetic is a saturable process. At a high HuMV833 plasma concentration (811 μg/mL), 50% inhibition of plasma clearance occurred. The safety of HuMV833 was evaluated in the same cynomolgus monkeys treated with 0, 1, 10, or 30 mg/kg of HuMV833, with essentially no treatment-related toxicity (data not shown). The study protocol was reviewed and approved by the Institutional Animal Care and Use Committee (IACUC) of Primedica Corporation (Worcester, MA) before the start of the study.

Patients

Patients who had progressive solid tumors that were not amenable to standard therapies were eligible for the study. Patients were included in the study if they had a life expectancy of at least 3 months and an Eastern Cooperative Oncology Group (ECOG) performance status less than or equal to 2 *(17).* Inclusion criteria required that patients be at least 18 years of age, have a minimum neutrophil count of 1.5×10^9/L, a minimum platelet count of 100×10^9/L, a minimum hemoglobin concentration of 10 g/dL, a serum bilirubin level of less than 1.5 times the upper limit of normal, serum transaminase levels of less than 2.5 times the upper limit of normal, a serum creatinine level of less than 120 μg/mL (1.4 mg/dL), and have normal prothrombin time and activated partial thromboplastin time (APTT) coagulation measurements. All patients had a normal 12-lead electrocardiogram. The patients did not have any unstable systemic disease, used adequate contraception, or did not have reproductive potential.

Patients were excluded from the study if they were known to have the human immunodeficiency virus, hepatitis B virus, or brain metastases. Patients were also excluded if they had finished a previous treatment (surgery, chemotherapy, immunotherapy, or radiotherapy) less than 4 weeks before entering the study, had not recovered from previous treatment toxicities, or currently had or had previously had a second malignancy. Any patient currently taking steroids was also excluded. Twenty patients entered the study between January 2000 and March 2001.

The protocol was written by G. Jayson on behalf of the European Organization for Research and Treatment of Cancer (EORTC) Biological Therapeutic Development Group and was approved by the EORTC protocol review committee (EORTC 13992). HuMV833 was supplied by Protein Design Labs., Inc., and approved by the medicines control agency in each participating country. Each of the four participating centers (Christie Hospital, Manchester, U.K.; Academisch Ziekenhuis Maastricht, Maastricht, The Netherlands; Universitair Medisch Centrum Utrecht, Utrecht, The Netherlands; Linkoping University Hospital, Linkoping, Sweden) gained approval from its local research ethics committee. All patients gave written informed consent and the trial was performed according to Good Clinical Practice regulations. The project was also approved by the U.K. Administration of Radioactive Substances Advisory Committee (ARSAC).

Trial Design

The trial was an open label, multiple dose, dose escalation phase I study in which the antibody was administered in 0.9% saline (up to 250 mL) over 1 hour on days 1, 15, 22, and 29. A minimum of three patients were accrued at each dose level (0.3, 1, 3, and 10 mg/kg). Toxicity was evaluated by using criteria from the National Cancer Institute of Canada Common Toxicity Criteria (version 2). Tumor response was determined clinically and radiologically by using the RECIST criteria *(18).* A staging computed tomography (CT) scan was performed during the 2 weeks before treatment began and between days 29 and 36 after the first infusion of HuMV833. Patients who had stable disease or better after day 35 were permitted to continue on the same weekly dose of antibody for up to 6 months.

Successive dose levels were opened for accrual if no patient in the preceding cohort had experienced a grade III or grade IV toxicity. If the latter occurred, then an additional three patients were entered at that dose level. The maximum tolerated dose was defined as the last dose at which at least five of six patients did not experience a grade III or grade IV toxicity.

PET: Radiolabeling and Characterization of ^{124}I-HuMV833

Iodine-124 (half-life = 100 hours) was produced by cyclotron irradiation of enriched tellurium-126 targets and extracted by dry distillation. Clinical grade ^{124}I-HuMV833 was prepared by direct labeling using chloramine-T as a mild oxidant. The overall radiochemical yield, after purification, was 75.8% ± 13.5%. The specific activity was 150–300 MBq/mg of protein. Size exclusion gel chromatography showed that the radiolabeled protein was stable in patient plasma throughout the imaging study (data not shown). The antibody was labeled in a clinical grade laboratory (Paterson Institute, Manchester, U.K.) under aseptic conditions.

The binding affinity of the ^{124}I-HuMV833 and the unlabeled HuMV833 protein to VEGF was determined by measuring the affinity constant (K_a) of monoclonal HuMV833 to VEGF in solution by an indirect competition ELISA *(20).* In brief, varying amounts of HuMV833 (0.01–10 μg/mL) were incubated at 4 °C for 16–18 hours with 200 ng/mL VEGF in solution (1% bovine serum albumin, 0.05% Tween 80 in phosphate-buffered saline [PBS]) until equilibrium was reached. The remaining unbound VEGF was captured by plate-bound monoclonal HuMV833 (0.1 μg/mL, 100 μL in borate-buffered saline) and quantified by ELISA using a goat anti-VEGF polyclonal antibody (100 μL of a 200 ng/mL solution; R&D Systems, Abingdon, U.K.). The ELISA was developed with an HRP-conjugated rabbit anti-goat antibody (1 : 3000 dilution; DAKO, Glostrup, Denmark), with tetramethyl benzidine (0.1 mg/mL; Sigma Chemical Co., Poole, U.K.) as the chromogen. At equilibrium, 50% saturation of plate-bound antibody corresponds to the dissociation constant of the competing antibody. The affinity constant is the reciprocal of the dissociation constant *(19).*

The affinity constant of unlabeled HuMV833 and ^{124}I-labeled HuMV833 to VEGF before infusion was $1.8 \times 10^8\ M^{-1}$ and $1.25 \times 10^8\ M^{-1}$ (N = 7), respectively, demonstrating retention of binding affinity of the ^{124}I-HuMV833 to VEGF (Fig. 1). Intact HuMV833 was recovered from one patient treated with 1 mg/kg (data not shown), confirming that VEGF-binding potential was retained following iodination and administration to patients.

PET Imaging

The PET study was conducted in patients treated in Manchester, U.K. ^{124}I-HuMV833 (1 mg) was mixed with the unlabeled therapeutic HuMV833 antibody during the first treatment cycle and administered over 1 hour. The average dose administered

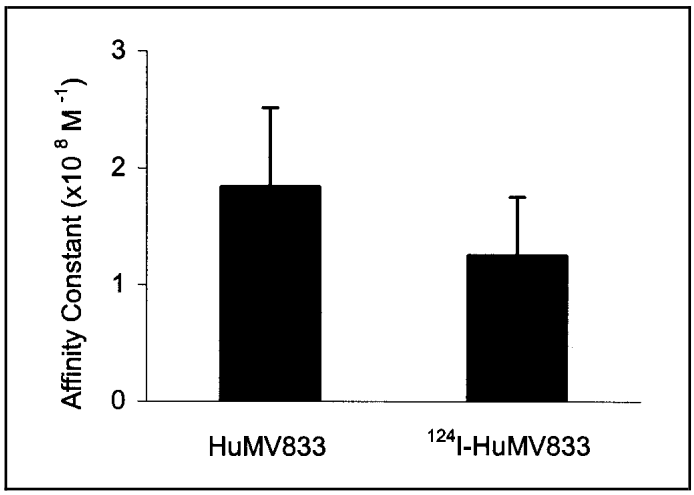

Fig. 1. Comparison of the association constants (K_a) of the unlabeled and ^{124}I-labeled humanized anti-vascular endothelial growth factor (VEGF) antibody HuMV833 were compared by using an ELISA. The K_a was calculated from the mean of six experiments. The graph shows the mean K_as with 95% confidence intervals.

intravenously to the six patients in the PET study was 80 MBq, with an effective dose of 0.3 mSv/MBq.

Patients received oral Lugol's iodine for 48 hours before administration of the PET reagent to minimize uptake of the ^{124}I-HuMV833 by the thyroid. PET imaging was performed approximately 24 and 48 hours after the infusion using a GE Advance PET scanner (General Electric Medical Systems, Milwaukee, WI), a full-ring Bismuth Germanate (BGO)-based PET scanner, with an axial field-of-view of 15 cm producing 35 slices of a 4.25-mm thickness. Imaging was typically done as three contiguous blocks covering the chest, abdomen, and pelvis, with 20-minute emission and 10-minute transmission (for attenuation correction) scans per section, i.e., approximately 1.5 hours to cover a distance of 45 cm. Emission scanning was performed in 2-D mode, which accurately quantified the images with acceptable correction for random and scatter events (residual errors <3%). Absolute quantitative calibration of activity levels in the reconstructed images (in kBq/mL) was ensured by using a separate well counter calibration performed in the standard way but using an accurately measured solution of ^{124}I. Images were reconstructed into 128- × 128-pixel matrices corresponding to 55-cm^2 sections, with both analytic and iterative reconstruction, using segmented attenuation correction. Analytic reconstructions via filtered back-projection were performed with a 12-mm Hanning filter (72% of the Nyquist frequency). Iterative reconstructions were done by using the ordered-subset expectation-maximization (OSEM) method *(20),* with post-filtering using a 10-mm wide Gaussian filter.

Magnetic Resonance Evaluation of Vascular Permeability

The magnetic resonance study was conducted in patients treated in Manchester, U.K. VEGF produces rapid and substantial increases in vascular permeability. MRI was used to test the hypothesis that effective biologic activity of the anti-VEGF antibody would result in detectable reductions in endothelial permeability within tumor vessels. We used dynamic MRI to produce quantified parametric images of the endothelial permeability surface area product (k^{trans}) and of the relative tumoral blood volume *(21).* To eliminate respiratory artifacts in the images, we used breath-hold image acquisition combined with a novel pharmacokinetic model to allow estimation of k^{trans} and relative tumoral blood volume from measurements made during the first passage of a contrast bolus through the tumor vascular bed *(22).* To distinguish measurements made with this technique from those made with conventional approaches, we refer to the calculated k^{trans} as k_{fp} (transfer coefficient for the first pass) *(23).*

Magnetic resonance images were acquired before first treatment, 48 hours after first treatment, and after four infusions of treatment (7–14 days after the last treatment, approximately day 35). Magnetic resonance images were obtained on a 1.5 T Philips ACS NT-PT6000 scanner (Philips Medical Systems, Best, The Netherlands). Routine pre-contrast T1 and T2 weighted and post-contrast T1 weighted images were acquired to allow identification of the tumor. The imaging protocol for dynamic contrast enhanced studies consisted of three consecutive 3-D rf-spoiled (T1-weighted) field echo acquisitions with flip angles of 2°, 10°, and 35° to allow calculation of T1 maps *(25).* The third imaging sequence was repeated to produce a T1-weighted dynamic data set with a time resolution of 5.1 seconds and a duration of 1 minute. Contrast agent (0.1 m*M*/kg of gadodiamide: Gd-DTPA-BMA) was given intravenously by power injector over a period of 4 seconds via a 16-gauge cannula inserted into an antecubital vein as the imaging sequence commenced.

Image data were analyzed in four steps. First, dynamic data were reviewed to exclude patients who moved substantially during image acquisition. Second, baseline maps of true T1 were calculated by using the three images with varying flip angles. Third, an arterial input function was manually identified from the dynamic series. Fourth, relative tumoral blood volume and k^{trans} were calculated pixel by pixel for the entire data set on the basis of the changes in contrast concentration during the first passage of the contrast bolus. The calculation of k_{fp} and relative tumoral blood volume uses an iterative fitting technique *(22)* that decomposes the intra- and extravascular components of the signal change during the passage of the contrast bolus.

Image Analysis

Two experienced radiologists (J. Lawrance and A. Jackson) and a physicist (P. Julyan) defined regions of interest (ROI) of tumor and normal tissue on the patients' CT scans. For PET images, the ROI were defined from the iterative PET and analytic reconstructions. Results were expressed in terms of either the percentage of injected dose per gram (%id/g), normalized to the administered activity, or the antibody concentration in μg/mL, knowing the therapeutic dose given to each patient. For MRIs, the ROI were subsampled to exclude nonenhancing tissue by identifying pixels that showed a signal increase of 20% or greater between pre- and post-contrast T1-weighted magnetic resonance scans. These ROI were then applied to parametric maps to extract mean and standard deviations of k_{fp} and relative tumoral blood volume.

Pharmacokinetic Assessment of HuMV833

Plasma samples were collected from each patient before treatment (day 0); on the treatment day (day 1) at 5 minutes and at 1, 3, 6, 24, and 72 hours; at 7 and 10 days after the first infusion and the fourth infusion (which took place on day 29); before and 6 hours after the second and third infusions (which took place on days 15 and 22); on days 39 and 43; and at 3 months. To isolate plasma, whole blood was collected from each patient in tubes

containing a 3.8% sodium citrate solution. The blood was centrifuged within 24 hours of collection to extract the plasma samples, which were then stored at –80 °C until assayed.

Plasma concentrations of HuMV833 were determined by using the specific antibody-captured ELISA (Protein Design Labs, Inc.) with $VEGF_{165}$ as the solid-phase capture reagent, as described earlier for the preclinical pharmacokinetic profile. All calibrators and controls were stored frozen at a maximum of –60 °C until use.

The plasma concentrations of HuMV833 were used to construct concentration–time profiles. Biexponential equations were fitted to the weighted plasma concentration–time data from each patient using nonlinear least squares regression analysis (WinNonlin; Pharsight, Mountain View, CA). The coefficients and exponents of the biexponential equations were used to calculate the following pharmacokinetic parameters: area under concentration versus time curve (AUC), highest measured concentration (C_{max}), clearance (CL), half-life of HuMV833 ($t_{1/2}$), volume of distribution in the central compartment (V_c), and the steady-state volume of distribution (V_{ss}) *(25,26).*

Total Plasma VEGF Concentration

Plasma samples were collected from all patients for total VEGF measurements before treatment (day 0); at 5 minutes, at 1, 6, and 24 hours, and at 7 days after the first infusion; before and 6 hours after each subsequent infusion (which took place on days 15, 22, and 29); and on day 43. Plasma concentrations of total VEGF were determined with a sandwich ELISA kit (R&D Systems, Abingdon, U.K.), according to the manufacturer's recommended protocol, with the exception that pooled normal human plasma was substituted for the calibrator diluent in the kit. The molar ratio was calculated (assuming the molecular weight of HuMV833 was three times of that of the VEGF) as follows:

$$\text{HuMV833/VEGF molar ratio} = [\text{HuMV833 concentration (ng/mL)} \times 1000]/[3 \times \text{VEGF concentration (pg/mL)}]$$

The quantitative range of the assay was 50–1800 pg/mL, with a detection limit of 31.25 pg/mL. The ELISA accuracy ranged between 82% and 113%. The precision was estimated to be less than 10% across the quantitative range.

Results

Patients

Twenty patients were entered into this phase I study to evaluate the distribution and biologic effects of HuMV833. The median age of the patients was 51.5 years and the median ECOG score was 1. Six of the patients included in the study had been diagnosed with colorectal cancer, five with ovarian cancer, two with breast carcinoma, two with melanoma, one with angiosarcoma, one with neuroblastoma, one with laryngeal cancer, one with osteosarcoma, and one with metastatic carcinoma of unknown primary. All patients had undergone initial surgery and had received chemotherapy and/or radiotherapy, depending on their disease.

Of the 20 patients, four patients were treated with HuMV833 at dose level 1 (0.3 mg/kg), six at dose level 2 (1 mg/kg), six at dose level 3 (3 mg/kg), and four at dose level 4 (10 mg/kg). Nineteen patients were evaluable. For most patients, HuMV833 was nontoxic and well tolerated, with nine patients continuing treatment beyond the first four doses and two patients gaining clinically significant benefit. One patient with ovarian cancer attained a good partial response that lasted for 31 weeks, whereas another with colon cancer had stable disease for 15 months.

PET Pharmacokinetic Evaluation of HuMV833

^{124}I-HuMV833 (1 mg) was administered with the rest of the unlabeled HuMV833 treatment dose during the first treatment. Although three patients were treated per dose level, we randomly selected two patients from each group for analysis. We evaluated two patients, one with ovarian cancer and one with colon cancer, who received 1 mg/kg; two patients, one with neuroblastoma and one with ovarian cancer, who received 3 mg/kg; and two patients, one with colon cancer and one with ovarian cancer, who received 10 mg/kg.

HuMV833 uptake between and within patients, as analyzed by PET, was highly variable (representative PET images shown in Fig. 2). The HuMV833 concentration in the pelvic deposit of a patient with ovarian cancer (3.2 μg/mL) was similar to that in other tissues in the same patient (range = 2.4 μg/mL–4.1μg/mL) (Fig. 2, A). The HuMV833 concentration in the tumor deposit in a poorly vascularized metastasis from colon cancer (5.1 μg/mL) (Fig. 2, B) was substantially less than that present in the patient's liver (18.7 μg/mL). The HuMV833 concentration in the neck mass of a patient with metastatic neuroblastoma was substantially less than that in the anterior mediastinal mass at 24 hours (6.9 μg/mL versus 12.1 μg/mL, respectively) (Fig. 2, C) and 48 hours (5.7 μg/mL versus 11.0 μg/mL, respectively) (Fig. 2, D). The largest range in HuMV833 concentration in tumor deposits in a single patient was seen in a patient with ovarian cancer who received the 3-mg/kg dose. One tumor deposit contained 1.7 μg/mL HuMV833 at 24 hours and another contained 5.8 μg/mL HuMV833 at 24 hours, a 3.4-fold difference. These data show that the distribution of this humanized monoclonal antibody differed in different parts of the body and in different tumor deposits.

We also compared HuMV833 concentrations and clearance in normal tissues. A comparison of the amount of ^{124}I-HuMV833 present after 24 and 48 hours showed that, whereas different normal tissues cleared the antibody at approximately equal rates, clearance rates in different tumor deposits varied widely (Fig. 3). The wide variation was seen even in individual patients. The largest range within a patient with respect to a reduction in antibody concentration between 24 and 48 hours was 16% in one tumor deposit and 75% in another tumor deposit. This occurred in a patient with ovarian cancer who received a 3-mg/kg dose of antibody.

Magnetic Resonance Evaluation of k_{fp}, the Vascular Permeability Surface Area Product

Because VEGF regulates vascular permeability and HuMV833 inhibits VEGF *in vitro,* we hypothesized that HuMV833 would reduce vascular permeability *in vivo.* Magnetic resonance determinations of k_{fp}, the vascular permeability surface area product, were performed before treatment, 48 hours after treatment, and at day 35 (6 days after the final drug administration). Representative color-enhanced images are shown in Fig. 4, A and B.

We detected changes in tumoral k_{fp} in all patients at each of the antibody doses (Fig. 4, C). All patients had a substantial decrease in k_{fp} at 48 hours (median = 44%, range = 5%–91%).

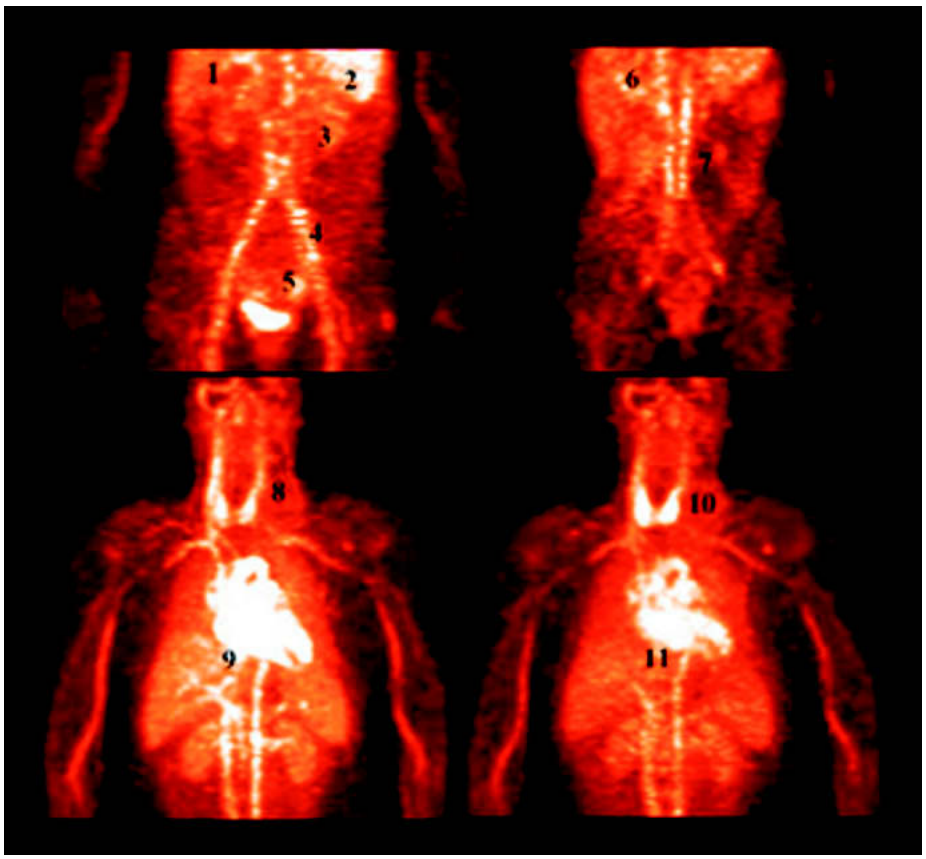

Fig. 2. Positron emission tomography (PET) evaluation of the distribution and intratissue concentration of the ^{124}I-labeled humanized anti-vascular endothelial growth factor (VEGF) antibody HuMV833. Two patients at each of the dose levels (1, 3, and 10 mg/kg) were injected with 70 MBq (1 mg) of ^{124}I-HuMV833 together with unlabeled HuMV833 during the first cycle of administration of the antibody. PET was performed approximately 24 and 48 hours after administration, regions of interest were drawn on the PET images, and the percentage of radioactivity in each tissue volume was measured to calculate the concentration of antibody present in that tissue. Representative PET images are shown. **A**) Image taken after 24 hours of a patient with a pelvic deposit of ovarian cancer who received 1 mg/kg HuMV833 with ^{124}I-HuMV833. Similar antibody concentrations were detected in the (**1**) liver (2.4 μg/mL), (**2**) spleen (4.1 μg/mL), (**3**) left kidney (2.8 μg/mL), (**4**) femoral artery (3.0 μg/mL), and (**5**) pelvic ovarian cancer deposit (3.2 μg/mL). **B**) Image taken after 24 hours of a patient with a poorly vascularized metastasis from colon carcinoma who received 10 mg/kg HuMV833 with ^{124}I-HuMV833. Substantial differences in the antibody concentration were detected in the (**6**) liver (18.7 μg/mL) and (**7**) poorly vascularized para-aortic colon carcinoma metastasis (5.1 μg/mL). **C**) Image taken after 24 hours of a patient with metastatic neuroblastoma who received 3 mg/kg of HuMV833. Different antibody concentrations were detected in two different tumor deposits: the (**8**) left neck neuroblastoma metastasis (6.9 μg/mL) and (**9**) anterior mediastinal neuroblastoma metastasis (12.1 μg/mL). **D**) Image taken after 48 hours of the same patient as shown in **C.** Different antibody concentrations were still detected in the two different tumor deposits (**10**) left neck neuroblastoma mass (5.7 μg/mL) and (**11**) anterior mediastinal neuroblastoma mass (11.0 μg/mL). The color intensities for the images shown in **C** and **D** have been adjusted for the decay of the ^{124}I and are therefore comparable. The color intensities for the other images cannot be directly compared with each other. The numbers in parentheses refer to the **black** numbers on the images.

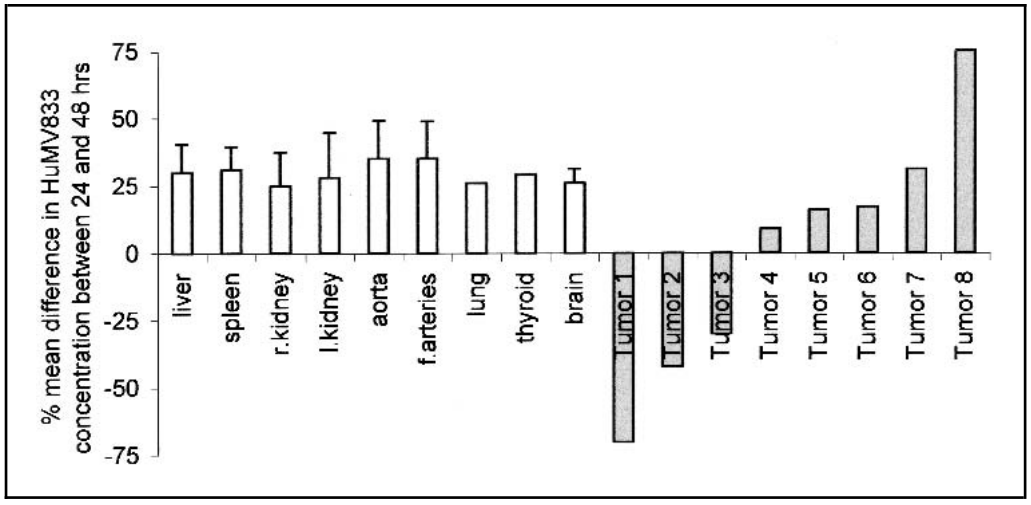

Fig. 3. Comparison of the difference in the concentration of ^{124}I-labeled humanized anti-vascular endothelial growth factor (VEGF) antibody HuMV833 in normal (**open bars**) and malignant tissues (**gray bars**) between 24 and 48 hours after administration of the antibody. The amount of antibody present in tissues was calculated on the basis of positron emission tomography (PET) images collected at 24 and 48 hours after administration of ^{124}I-HuMV833. For normal tissues, the **bars** represent the mean difference in antibody concentration for all 19 evaluable patients, with 95% confidence intervals. For malignant tissues, the **bars** represent individual values for different tumor masses imaged in different patients. Tumor numbers refer to individual tumor masses in patients with the following diseases and treated at particular dose levels: tumor 1–colon cancer, 1 mg/kg; tumor 2–colorectal cancer, 10 mg/kg; tumor 3–neuroblastoma, 3 mg/kg; tumor 4–neuroblastoma, 3 mg/kg; tumor 5–ovarian cancer, 3 mg/kg; tumor 6–neuroblastoma, 3 mg/kg; tumor 7–ovarian cancer, 10 mg/kg; tumor 8–ovarian cancer, 3 mg/kg. Tumors 3, 4, and 6 were identified in the same patient. Tumors 5 and 8 were identified in the same patient.

Absolute values of k_{fp} varied greatly from one patient to another, with an order of magnitude difference in baseline (pretreatment values). We did not observe a dose–k_{fp} relationship between patients receiving different antibody dose levels (Fig. 4, C). However, when we examined the data for a particular patient, the k_{fp} value at 48 hours in 11 of 12 measurements in individual patients was less than that at 35 days, which is consistent with a concentration–response relationship. Fig. 4, C, also shows that, unlike k_{fp} responses at higher antibody doses, the change in k_{fp} at a dose of 0.3 mg/kg at 48 hours was not sustained on the day 35 scan.

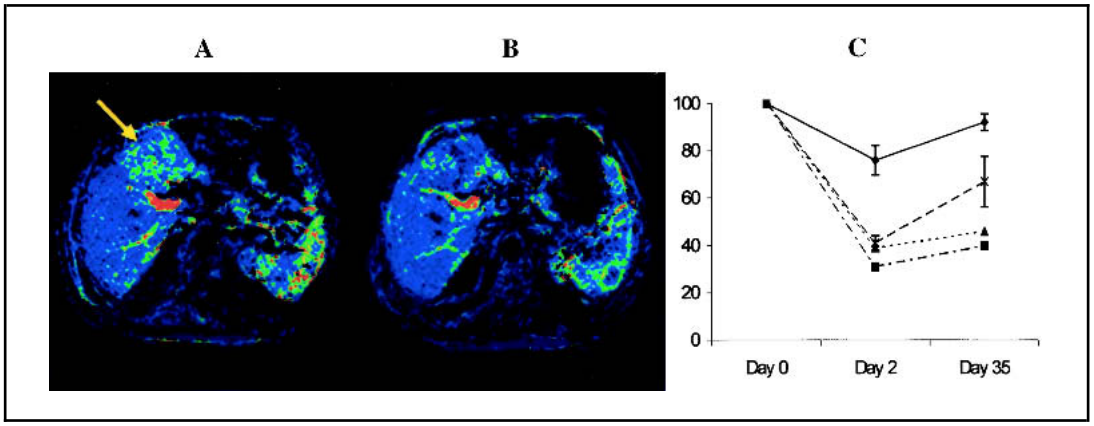

Fig. 4. Magnetic resonance images were used to determine tumor endothelial permeability surface area product k_{fp} before (**A**) and after (**B**) patients were treated with the humanized anti-vascular endothelial growth factor (VEGF) antibody HuMV833. Representative images are shown in (**A**) and (**B**). **A**) The magnetic resonance image showing the k_{fp} of a metastasis (**yellow arrow**) in the left lobe of the liver in a patient before receiving HuMV833 (1 mg/kg). **B**) The magnetic resonance image showing the vascular permeability of the same metastasis from the same patients 48 hours after receiving HuMV833. The areas of **green** and **blue** represent high and low vascular permeability, respectively. **Red** and **yellow** pixels represent artifactually high measurements in the hepatic vein. **C**) The k_{fp} of representative tumors was determined for all patients before treatment, 2 days after the first treatment was initiated, and 35 days after the first treatment was initiated. The vascular permeability of the tumor after treatment was compared with that before treatment, and the data were expressed as the mean percent change relative to the value before treatment for each different treatment dose level, with 95% confidence intervals. Each treatment dose level is represented by a different symbol. **Solid diamonds** = 0.3 mg/kg; **solid squares** = 1 mg/kg; **solid triangles** = 3 mg/kg; **crosses** = 10 mg/kg. The permeability measurement is k_{fp} (min^{-1}).

Co-registration (Superimposition) of PET and Magnetic Resonance Data

The PET and magnetic resonance data allowed us to test the hypothesis that regional vascular permeability was associated with the antibody localization in the tumor. The results are illustrated in Fig. 5, in which affine image co-registration has been performed between magnetic resonance-derived maps of k_{fp} and PET data in a woman with a pelvic deposit of ovarian cancer. The data show that the distribution of antibody, as estimated by PET, was qualitatively associated with the regional vascular permeability and the distribution of k_{fp}. Differences in axial rotation and nonlinear distortions precluded a quantitative analysis of co-registered data.

Plasma Pharmacokinetics of HuMV833 and Serum VEGF Concentration

We determined the mean plasma concentration of HuMV833 in patients treated at each dose level (Fig. 6) and used that

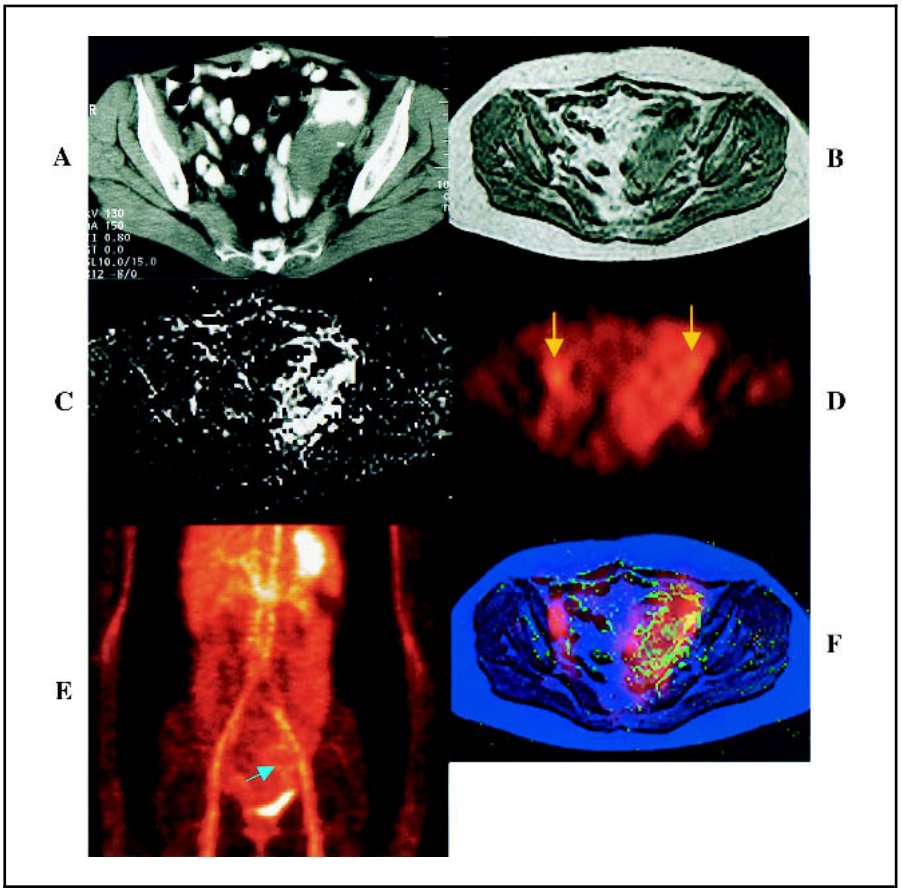

Fig. 5. Co-registration (superimposition) of positron emission tomography (PET)–pharmacokinetic and magnetic resonance–pharmacodynamic measurements. Axial images through the same level of the pelvis of a woman with a deposit of ovarian cancer who received the humanized anti-vascular endothelial growth factor (VEGF) antibody HuMV833 (10 mg/kg) are shown in parts **A–D** and **F. A**) A contrast-enhanced computed tomographic scan image with a deposit of ovarian cancer identified (**red arrow**). **B**) The T1-weighted magnetic resonance image of the same region of the pelvis as shown in **A. C**) The vascular permeability (k_{fp} [min^{-1}]) map of the same section of the pelvis. High vascular permeability is represented by **white** pixels. The tumor is the most permeable structure in the pelvis. **D**) The PET distribution of HuMV833 in same region of the pelvis as shown in **A.** The symmetrical uptake (**yellow arrows**) of antibody in the pelvis results from antibody in the femoral vessels. **E**) The maximum intensity projection anterior-posterior (AP) view in which the patient's tumor appears as a ring-enhancing lesion in the left pelvis (identified by the **blue arrow**). **F**) The co-registered (merged) images of T1-weighted magnetic resonance are shown in **blue,** the magnetic resonance-determined vascular permeability in green, and the PET-determined antibody distribution in **red.**

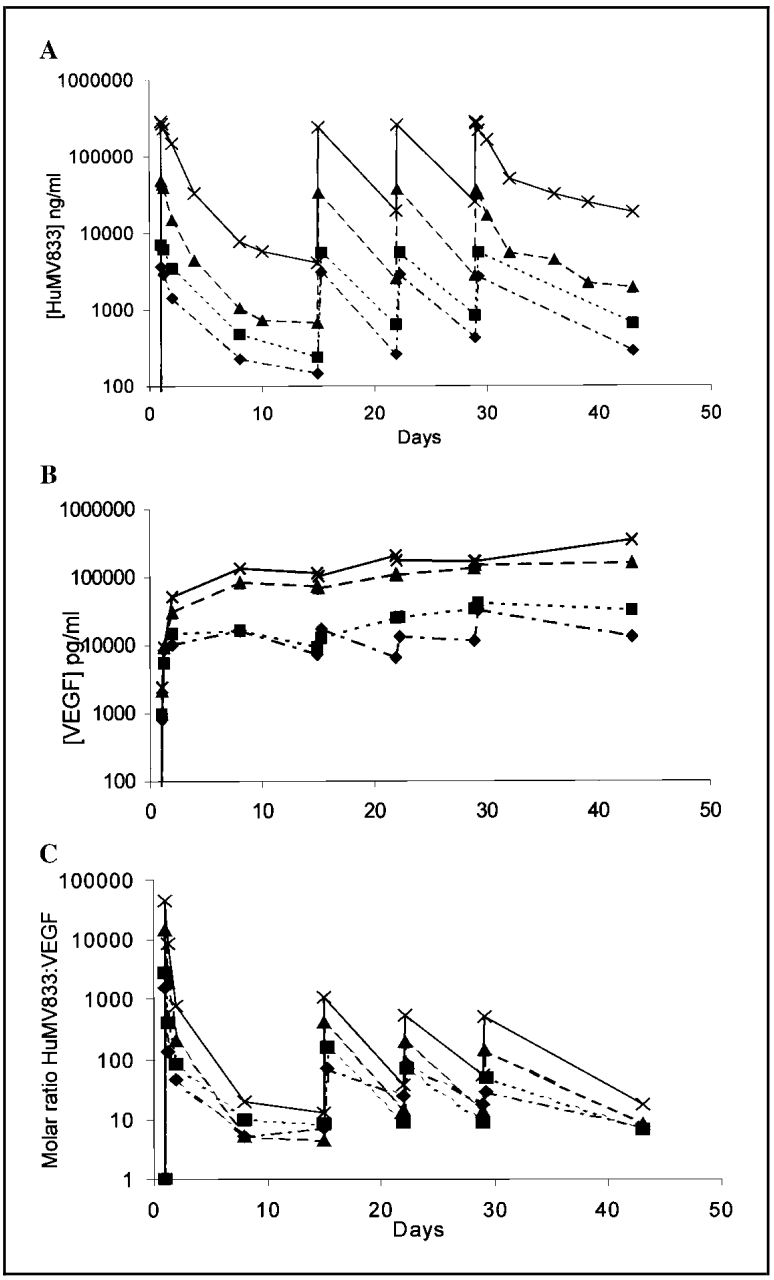

Fig. 6. Plasma pharmacokinetics (concentration versus time) of the humanized anti-vascular endothelial growth factor (VEGF) antibody HuMV833 (**A**), plasma total VEGF (**B**), and the ratio of HuMV833 to total VEGF (**C**). Plasma samples were taken from all patients at a number of time points during the trial, and the concentration of HuMV833 was determined by enzyme-linked immunosorbent assay (ELISA). The total plasma VEGF concentrations were determined simultaneously by using a VEGF-specific ELISA. The molar ratio of HuMV833 antibody concentration to VEGF was determined. HuMV833 was intravenously administered to patients on days 1, 15, 22, and 29. Each curve represents the mean values for all patients who received a specific dose level. **Solid diamonds** = 0.3 mg/kg; **solid squares** = 1 mg/kg; **solid triangles** = 3 mg/kg; and **crosses** = 10 mg/kg.

information to determine pharmacokinetic data for HuMV833 (Table 1). The most important finding is that there was no clear relationship between plasma pharmacokinetics and PET-determined clearance of HuMV833 from tumors over the 24- to 48-hour PET study, suggesting that the former cannot be used as a surrogate for the latter.

The total (antibody-bound and free) plasma VEGF concentration measured in all patients (Fig. 6, B) showed a severalfold increase in circulating VEGF levels relative to pretreatment levels, but there appeared to be little difference in VEGF levels detected in patients who received the 3-mg/kg or 10-mg/kg HuMV833 dose. A comparison of the molar concentration of

Table 1. Plasma pharmacokinetics of the humanized anti-VEGF antibody HuMV833*

Dose group, mg/kg	N	C_{max}, μg/L	AUC, μg-h/L	V_c, L/kg	V_{ss}, L/kg	CL, L/h/kg	$T_{1/2}$, h
0.3	4	3748.4 ± 1987	187 664.6 ± 49 259	0.0680 ± 0.0706	0.3046 ± 0.141	0.00162 ± 0.0004	196 ± 141
1.0	6	6432.7 ± 3716	438 903.5 ± 267 731	0.1584 ± 0.0696	0.7009 ± 0.388	0.00239 ± 0.0012	326 ± 237
3.0	6	46 510.0 ± 37 788	1 949 261.8 ± 1 461 648	0.0690 ± 0.0544	0.3688 ± 0.245	0.00171 ± 0.0017	333 ± 384
10.0	4	401 101 ± 250 875	32 597 417.9 ± 31 359 377	0.0268 ± 0.017	0.1681 ± 0.37	0.00045 ± 0.0006	448 ± 1009

*AUC = area under concentration versus time curve; C_{max} = highest measured concentration; CL = clearance; $t_{1/2}$ = half-life of HuMV833; V_c = volume of distribution in central compartment; V_{ss} = steady state volume of distribution; VEGF = vascular endothelial growth factor.

†Mean plasma pharmacokinetic (± 95% confidence intervals) values for all patients entered at each dose level.

antibody and total VEGF at all time points revealed that there was nearly always at least five times more antibody than total cytokine.

Discussion

There has been a worldwide research program to develop antiangiogenic agents for the treatment of cancer. Many families of antiangiogenic drugs now exist, but their clinical development has been hampered by a paucity of data concerning the optimum biologically active dose. In addition, although the classical phase I study design focuses on toxicity as an endpoint to establish the maximum tolerated dose, many humanized monoclonal antibodies have no clinically significant toxicity, which precludes identification of the maximum tolerated dose. Furthermore, biologic dose–response relationships may follow a bell-shaped curve *(27),* and therefore the maximum tolerated dose may not even be the best dose for clinical applications. To overcome these issues, biologic pharmacodynamic investigations *(28)* have entered phase I clinical trial design with the goal of establishing the optimum biologically active dose. However, the present study has shown that tumor deposits, even within the same patient, can behave differently with respect to drug uptake, drug clearance, and biologic response. Thus, it is difficult to establish a standard dose in the way that is practiced for most cytotoxic agents.

In this study, we radiolabeled the anti-VEGF antibody HuMV833 with ^{124}I and performed the first PET–pharmacokinetic study of an antiangiogenic agent. The labeled antibody was co-administered with unlabeled antibody to all patients, and the percentage of uptake of the radiolabel allowed us to calculate the amount of total antibody (labeled and unlabeled) in the patients' tumors and organs. The concentration of HuMV833 in tumor deposits within an individual patient varied by more than threefold, whereas the reduction in drug concentration in a patient's tumor deposits ranged between 16% and 75% over a 24-hour period. In one patient with neuroblastoma who received 3 mg/kg of HuMV833, one tumor deposit accumulated HuMV833 over the 24-hour study period, while another cleared the antibody. By contrast, normal organs and tissues cleared the antibody at approximately equal rates. Thus, the PET–pharmacokinetic study has shown that different tumor deposits in the same patient can take up and clear HuMV833 in different ways. The differences in drug distribution and clearance could lead to clinically important differences in tumor exposure to HuMV833 and may contribute to the apparent lack of clinical activity of certain tumor deposits to the antibody. Although our observations may be relevant to other monoclonal antibodies in the clinic, whether these factors (e.g., variation in drug distribution, drug clearance, baseline variation in vascular permeability and response) impair drug efficacy when smaller molecular weight antiangiogenic drugs are considered remains to be established.

We used magnetic resonance algorithms to measure k_{fp}, the vascular permeability surface area product, a parameter that is controlled by VEGF, and one we anticipated would decrease if the antibody was biologically active. We had previously shown these algorithms to be reproducible *(22),* and the differences in pretreatment versus maximum reduction in k_{fp} that we recorded here exceeded 15%, which was the established coefficient of variance for liver metastases, suggesting that the antibody was biologically active. The k_{fp} maps of the patients' tumors showed distinct anatomic variation, suggesting that k_{fp}, and therefore perhaps VEGF activity, varies from one area to another. The variability was noticeable not only within tumors but also between patients, because the baseline permeability measurements across all patients varied by a factor of 10.

Taken together, these data reveal a marked variation in functional anatomy and pathophysiology within human tumors. The implication is that it is inappropriate to compare the biologic response of a patient with one tumor histology, treated with a particular dose of antibody, with another patient with another or even the same tumor type who received a different dose. The difference in biology may prevent any observation of a dose–response effect. If pharmacodynamic endpoints are to be used to identify the optimum biologically active dose, then two strategies may be needed to deal with these functional anatomic issues. The variation in biology could be controlled for by treating a cohort of patients with an intra-patient dose escalation strategy and applying the pharmacodynamic measurements to the same tumor mass, which is thereby exposed to different antibody concentrations. Such a cohort would not replace the existing phase I trial design, which identifies pharmacokinetics (including saturation of clearance upon prolonged exposure), dose-limiting toxicity, and the maximum tolerated dose but would be an additional part of the phase I trial design and one that might be appropriate for cytostatic antiangiogenic agents. Data from this study support the adoption of this intra-patient dose escalation strategy because greater permeability changes were seen 48 hours after the initiation of treatment than were seen at day 35, 6 days after the fourth treatment, implying that there is a concentration–response relationship within patients. A second strategy, which may be more suitable for drugs that have a long half-life with respect to tumor growth, would be to reduce the heterogeneity among patients by using stricter selection criteria and entering larger numbers of patients into conventional cohort-based phase I trials. Such selection parameters might include tumor histology, tumor size, and tumor location. This type of approach was used in an investigation of a VEGF receptor tyrosine kinase inhibitor *(28)* that revealed a dose–permeability relationship in the liver metastases of patients with metastatic colon carcinoma.

This study has revealed striking variation in human tumor behavior within individual patients, which may account for apparent resistance to antiangiogenic antibody therapies. Our observations have implications for future studies of cytostatic antiangiogenic agents. Whether it will be necessary to tailor individual therapy regimens to individual patients can be determined only in a randomized trial that compares the maximum tolerated dose-guided therapy with pharmacodynamically determined dosing.

References

(1) Neufeld G, Cohen T, Gengrinovitch S, Poltorak Z. Vascular endothelial growth factor (VEGF) and its receptors. FASEB J 1999;13:9–22.

(2) Gordon MS, Margolin K, Talpaz M, Sledge GW Jr, Holmgren E, Benjamin R, et al. Phase I safety and pharmacokinetic study of recombinant human anti-vascular endothelial growth factor in patients with advanced cancer. J Clin Oncol 2001;19:843–50.

(3) Margolin K, Gordon MS, Holmgren E, Gaudreault J, Novotny W, Fyfe G, et al. Phase Ib trial of intravenous recombinant humanized monoclonal antibody to vascular endothelial growth factor in combination with chemotherapy in patients with advanced cancer: pharmacologic and long-term safety data. J Clin Oncol 2001;19:851–6.

(4) Mendel DB, Schreck RE, West DC, Li G, Strawn LM, Tanciongco SS, et al. The angiogenesis inhibitor SU5416 has long-lasting effects on vas-

cular endothelial growth factor receptor phosphorylation and function. Clin Cancer Res 2000;6:4848–58.
(5) Laird AD, Vajkoczy P, Shawver LK, Thurnher A, Liang C, Mohammadi M, et al. SU6668 is a potent antiangiogenic and antitumor agent that induces regression of established tumors. Cancer Res 2000;60:4152–60.
(6) Wedge SR, Ogilvie DJ, Dukes M, Kendrew J, Curwen JO, Hennequin LF, et al. ZD4190: an orally active inhibitor of vascular endothelial growth factor signaling with broad-spectrum antitumor efficacy. Cancer Res 2000; 60:970–5.
(7) Drevs J, Hofmann I, Hugenschmidt H, Wittig C, Madjar H, Muller M, et al. Effects of PTK787/ZK 222584, a specific inhibitor of vascular endothelial growth factor receptor tyrosine kinases, on primary tumor, metastasis, vessel density, and blood flow in a murine renal cell carcinoma model. Cancer Res 2000;60:4819–24.
(8) Davidoff AM, Leary MA, Ng CY, Vanin EF. Gene therapy-mediated expression by tumor cells of the angiogenesis inhibitor flk-1 results in inhibition of neuroblastoma growth in vivo. J Pediatr Surg 2001;36:30–6.
(9) Yang JC, Haworth L, Steinberg SM, Rosenberg SA, Novotny W. A randomized double-blind placebo-controlled trial of bevacizumab (anti-VEGF antibody) demonstrating a prolongation in time to progression in patients with metastatic renal cancer [abstract No. 15]. Proc ASCO 2002;21.
(10) Marx GM, Steer CB, Harper P, Pavlakis N, Rixe O, Khayat D. Unexpected serious toxicity with chemotherapy and antiangiogenic combinations: time to take stock! J Clin Oncol 2002;20:1446–8.
(11) Asano M, Yukita A, Suzuki H. Wide spectrum of antitumor activity of a neutralizing monoclonal antibody to human vascular endothelial growth factor. Jpn J Cancer Res 1999;90:93–100.
(12) Herbst RS, Tran HT, Mullani NA, Charnsangavej C, Madden TL, Hess KR, et al. Phase I clinical trial of recombinant human endostatin (rHE) in patients (Pts) with solid tumors: pharmacokinetic (PK), safety and efficacy analysis using surrogate endpoints of tissue and radiologic response [abstract No. 9]. Proc ASCO 2001;20.
(13) Asano M, Yukita A, Matsumoto T, Hanatani M, Suzuki H. An anti-human VEGF monoclonal antibody, MV833, that exhibits potent anti-tumor activity in vivo. Hybridoma 1998;17:185–90.
(14) Queen C, Schneider WP, Selick HE, Payne PW, Landolfi NF, Duncan JF, et al. A humanized antibody that binds to the interleukin 2 receptor. Proc Natl Acad Sci U S A 1989;86:10029–33.
(15) Levitt M. Molecular dynamics of native protein. J Mol Biol 1983;168: 595–620.
(16) Sauer PW, Burky JE, Wesson MC, Sternard HD, Qu L. A high-yielding, generic fed-batch cell culture process for production of recombinant antibodies. Biotechnol Bioeng 2000;67:585–97.
(17) Oken MM, Creech RH, Tormey DC, Horton J, Davis TE, McFadden ET, et al. Toxicity and response criteria of the Eastern Cooperative Oncology Group. Am J Clin Oncol 1982;5:649–55.
(18) Therasse P, Arbuck SG, Eisenhauer EA, Wanders J, Kaplan RS, Rubinstein L, et al. New guidelines to evaluate the response to treatment in solid tumors. J Natl Cancer Inst 2000;92:205–16.
(19) Friguet B, Chaffotte AF, Djavadi-Ohaniance L, Goldberg ME. Measurements of the true affinity constant in solution of antigen-antibody complexes by enzyme-linked immunosorbent assay. J Immunol Methods 1985; 77:305–19.
(20) Hudson H, Larkin R. Accelerated image reconstruction using ordered subsets of projection data. IEEE Trans Med Imaging 1994;13:601–9.
(21) Tofts PS. Modeling tracer kinetics in dynamic Gd-DTPA MR imaging. J Magn Reson Imaging 1997;7:91–101.
(22) Jackson A, Haroon H, Zhu XP, Li KL, Thacker NA, Jayson G. Breath hold perfusion and permeability mapping of hepatic malignancies using magnetic resonance imaging and a first pass leakage profile model. NMR Biomed 2002;15:164–73.
(23) Li KL, Zhu XP, Waterton J, Jackson A. Improved 3D quantitative mapping of blood volume and endothelial permeability in brain tumors. J Magn Reson Imaging 2000;12:347–57.
(24) Zhu XP, Li KL, Kamaly-Asl ID, Checkley DR, Tessier JJ, Waterton JC, et al. Quantification of endothelial permeability, leakage space, and blood volume in brain tumors using combined T1 and T2* contrast-enhanced dynamic MR imaging. J Magn Reson Imaging 2000;11:575–85.
(25) Wagner JG. Linear pharmacokinetic equations allowing direct calculation of many needed pharmacokinetic parameters from the coefficients and exponents of polyexponential equations which have been fitted to the data. J Pharmacokinet Biopharm 1976;4:443–67.
(26) Gibaldi M, Perrier D. Pharmacokinetics. 1st ed. New York (NY): Marcel Dekker; 1982.
(27) Gruber BL, Marchese MJ, Kew R. Angiogenic factors stimulate mast-cell migration. Blood 1995;86:2488–93.
(28) Thomas A, Morgan B, Drevs J, Jivan A, Buchert M, Horsfield M, et al. Pharmacodynamic results using dynamic contrast enhanced magnetic resonance imaging of 2 Phase 1 studies of the VEGF inhibitor PTK787/ZK 222584 in patients with liver metastases from colorectal cancer [abstract No. 279]. Proc ASCO 2001;20.

NOTES

We thank G. Connolly for excellent data management and Dr. D. Lacombe and S. Mali at the EORTC for their help in running the trial. We are most grateful to Dr. Steve Keller, Dr. Junko Aimi, Yoshifumi Ota, and Han-Ting Ding for assay qualification and performance.

Manuscript received February 27, 2002; revised July 15, 2002; accepted July 25, 2002.